CEAS-GNC-2024-009

EuroGNC Navigation Guidance Control CEAS Bristol, UK June 11th-13th 2024
University of BRISTOL ROYAL AERONAUTICAL SOCIETY AIAA

Robust sliding mode controller design for orbital payload deploying spacecraft

Konstantinos Platanitis PhD Candidate, Cranfield University, SATM, MK43 0AL, Cranfield, United Kingdom. k.platanitis@cranfield.ac.uk

Dr. Leonard Felicetti Senior Lecturer, Cranfield University, SATM, MK43 0AL, Cranfield, United Kingdom. leonard.felicetti@cranfield.ac.uk

Dr. Saurabh Upadhyay Lecturer, Cranfield University, SATM, MK43 0AL, Cranfield, United Kingdom. saurabh.upadhyay@cranfield.ac.uk

Leonardo Capicchiano Lead AOCS Engineer, Coactum SA, Bex, Switzerland. leonardo.capicchiano@coactum.ch

ABSTRACT

This work demonstrates the feasibility of usage of a sliding mode controller in the case of orbital payload deployers. The proposed control law suggested herein allows for disturbance rejection during the payload deployment phase, as well as provide a basis for angular rate tracking purposes. The stability of the control law is determined by Lyapunov theory, and realistic spacecraft simulations have been created to verify the robustness in the presence of disturbances as well as the general tracking capabilities.

Keywords: Sliding mode control; Attitude control; Oribtal payload deployer

1 Introduction

Sliding mode control (SMC) has been introduced as a form of variable-structure control method since the 1960s [1] and has been studied in multiple disciplines, including space applications. This approach to control provides wanted features, such as fast response of dynamics, and low-to-no sensitivity towards uncertainties in plant modelling as well as towards external sources of disturbances. In general, SMC is a nonlinear control technique whose objective is driving a system towards a sliding condition, i.e. to slide on a phase-space defined surface. Such a control law is inherently discontinuous in time, as it switches between different control structures in accordance with the system's state with respect to the sliding surface. This discontinuity is obvious when referring to the output of the control law, and rapid switches are termed as "chattering". Despite the above drawbacks, studies of SMC applications in space include attitude control [2, 3], position and attitude control [4–6], and even extend to flexible structures [7–9].

Some of the characteristics of the SMC approach can be beneficial to the case of orbital payload deployers, namely the fast response times and the insensitivity towards plant uncertainties, which are a prerequisite when dealing with variable inertial properties that are changing within a small timeframe as is the case when the payload is separated from the body of the deployer spacecraft. Moreover, In this study the deploying mechanism is treated like a spring-release mechanism, where the payload will be thrusted away from the spacecraft body by pre-compressed springs which would impact a reaction force and thus a disturbance torque to the carrier craft. Since the mechanics of the release mechanism, as well

as the payload mass, are a priori known then this reaction force can be modelled and therefore bound. In this work, a control law is formulated under the pretense of a matching condition, that is driven by the upper limit of the bounded expected reaction torque during deployment.

Throughout the body of this work, system identification will be performed towards properly identifying the appropriate system dynamics, a sliding mode control law will be proposed by taking advantage of the matched uncertainty approach, and its stability will be proven by means of Lyapunov theory. To verify that such a control law actually performs as expected a simulation has been set up so as to emulate both realistic inputs to the controller from spacecraft sensors which will be sampled and discontinuous in time, as well as one possible solution to the control allocation problem is presented which takes into account the real spacecraft actuation capabilities, which the controller is unaware of.

2 System identification

Despite operating in space, and depending upon their altitude, spacecraft do experience various disturbances; from atmospheric drag to solar radiation pressure and the gravity gradient, there is an abundance of factors that would perturbe both their orbital as well as their attitude dynamics. While some of these effects have even been tried as possible control schemes, e.g. by trying to control the attitude by manipulating drag [10] or drag and gravity gradient [11], when accurate attitude maneuvering or orbital station-keeping is required on-board actuators that can provide thrusts and torques are employed.

In this work, the focus will be on spacecraft attitude control under extreme perturbations (i.e., payload deployment as compared to the aforementioned factors), and as far as the dynamics of the spacecraft are concerned they are modelled by the typical rigid body dynamics' equations:

$$I\dot{\bar{\omega}} = -(\bar{\omega} \times I\bar{\omega}) + \bar{M} \tag{1}$$

where I is the moment of inertia tensor, ω is the angular velocity in the body frame, $\bar{M}$ is the total torque applied to the body. As for the orbital dynamics, a simple model is used:

$$m\ddot{\bar{r}} = -\bar{\nabla}U \tag{2}$$

where m is the spacecraft mass, $\bar{r}$ is the position vector in ECI frame, and U is the gravitational potential expressed in the same frame.

Supposing that $I = diag([I_x, I_y, I_z])$ for the sake of convenience, then (1) can be decomposed as follows:

$$\begin{aligned} I_x\dot{\omega}_x &= (I_y - I_z)\omega_z\omega_y + M_x \\ I_y\dot{\omega}_y &= (I_z - I_x)\omega_x\omega_z + M_y \\ I_z\dot{\omega}_z &= (I_x - I_y)\omega_x\omega_y + M_y \end{aligned} \tag{3}$$

For simulation and control purposes it helps to define a state vector $x = [\omega_x, \omega_y, \omega_z]^T$ and this way eq. (3) becomes

$$\frac{d}{dt}\begin{bmatrix}\omega_x\\ \omega_y\\ \omega_z\end{bmatrix} = \begin{bmatrix}I_x^{-1}M_x + I_x^{-1}(I_y - I_z)\omega_y\omega_z\\ I_y^{-1}M_y + I_y^{-1}(I_z - I_x)\omega_x\omega_z\\ I_z^{-1}M_z + I_z^{-1}(I_x - I_y)\omega_x\omega_y\end{bmatrix} = I^{-1}\begin{bmatrix}M_x\\ M_y\\ M_z\end{bmatrix} + I^{-1}\begin{bmatrix}I_x^{-1}(I_y - I_z)\omega_y\omega_z\\ I_y^{-1}(I_z - I_x)\omega_x\omega_z\\ I_z^{-1}(I_x - I_y)\omega_x\omega_y\end{bmatrix} \tag{4}$$

3 Controller design

3.1 Control law

Eq (4) can be thought to describe an uncertain system of the form

$$\dot{x}(t) = Ax(t) + Bu(t) + f(x,u) \tag{5}$$

where the function $f : \mathbb{R} \times \mathbb{R}^n \times \mathbb{R}^m \rightarrow \mathbb{R}^m$ represents either uncertainty or non-linear behaviour in the system. If furthermore it holds that

$$f(t,x,u) = B\tilde{f}(t,x,u) \tag{6}$$

where again $\tilde{f} : \mathbb{R} \times \mathbb{R}^n \times \mathbb{R}^m \rightarrow \mathbb{R}^m$, and is not known but satisfies

$$||\tilde{f}(t,x,u)|| <= k||u|| + g(t,x) \tag{7}$$

where k is known and constrained to $1 > k >= 0$, and $g(t,x)$ is a known function, then f is said to satisfy the matching condition.

A control law with two parts (one linear and one non-linear) for the system represented in (4), given the matching condition constraints, is as follows

$$u(t) = u_L(t) + u_{NL}(t) \tag{8}$$

For the linear part, the following expression can be used, where Φ is any possible stable design matrix.

$$u_L(t) = -(SB)^{-1}(SA - \Phi S)x(t) \tag{9}$$

The non-linear part may be defined as follows:

$$u_{NL}(t) = -\rho(SB)^{-1}\frac{P\sigma(t)}{||P\sigma(t)||} \tag{10}$$

where ρ is a function of time and/or state, and $P \in \mathbb{R}^{m \times m}$ is a symmetric and positive definite matrix that satisfies the Lyapunov equation

$$P\Phi + \Phi^T P + I = 0 \tag{11}$$

For the scalar function ρ, any function can be used that satisfies the following, so it bounds the uncertain term $f(t,x,u)$

$$\rho(t,x) >= \frac{||SB||(k||u_L|| + g(t,x)) + \gamma}{1 - k||SB||||(SB)^{-1}||} \tag{12}$$

where $\gamma > 0$ is a design parameter of the controller.

Proof of the bounding action can be shown from (12) as follows:

$$\begin{aligned}\rho(t,x) &>= \|SB\|(k\|u_L\| + g(t,x)) + \gamma + k\|SB\|\|(SB)^{-1}\|\rho(t,x) \\ &>= \|SB\|(k\|u_L\| + g(t,x) + k\|(SB)^{-1}\|\rho(t,x)) + \gamma \\ &>= \|SB\|(k\|u\| + g(t,x) + \gamma \\ &>= \|SB\|\|\tilde{f}(t,x,u)\| + \gamma\end{aligned} \tag{13}$$

It is thus proven by (13) that $\rho(t,x)$ is greater than the matched uncertainty that appears in (6)

3.2 Stability

If the devised control law (8) as described by eqs. (9), (10) is substituted in (4), the dynamics of the sliding variables $\sigma = Sx$ become as follows:

$$\begin{aligned}\dot{\sigma}(t) &= (SA)x(t) + (SB)u + (SB)\tilde{f}(t,x,u) \\ &= \Phi\sigma - \rho(t,x)\frac{P\sigma}{\|P\sigma\|} + (SB)\tilde{f}(t,x,u)\end{aligned} \tag{14}$$

Choosing a Lyapunov candidate function such as $V = \sigma^T P\sigma$ stability can be guaranteed as follows:

$$\begin{aligned}\dot{V} &= \sigma^T(P\Phi + \Phi^T P)\sigma - 2\rho\|P\sigma\| + 2\sigma^T P(SB)\tilde{f} \\ &\leq \sigma^T(P\Phi + \Phi^T P)\sigma - 2\rho\|P\sigma\| + 2\|P\sigma\|\|(SB)\|\|\tilde{f}\| \\ &= -\sigma^T\sigma - 2\|P\sigma\|(\rho - \|SB\|\|\tilde{f}\|) \\ &\leq -\sigma^T\sigma - 2\gamma\|P\sigma\| \\ &\leq 0\end{aligned} \tag{15}$$

Thus, the stability of the proposed control law as constructed is proven and once the sliding phase is reached the σ-dynamics are independent of the uncertainty.

3.3 Application to spacecraft dynamics

Considering (4), we augment the system with sliding variables to get

$$\begin{aligned}\dot{x} &= Bu + B\tilde{f}(x) \\ &= \begin{bmatrix}\frac{1}{I_x} & 0 & 0 \\ 0 & \frac{1}{I_y} & 0 \\ 0 & 0 & \frac{1}{I_z}\end{bmatrix}\begin{bmatrix}M_x \\ M_y \\ M_z\end{bmatrix} + \begin{bmatrix}\frac{1}{I_x} & 0 & 0 \\ 0 & \frac{1}{I_y} & 0 \\ 0 & 0 & \frac{1}{I_z}\end{bmatrix}\begin{bmatrix}(I_y - I_z)x_2x_3 \\ (I_z - I_x)x_1x_2 \\ (I_x - I_y)x_1x_2\end{bmatrix} \\ \sigma &= Sx\end{aligned} \tag{16}$$

where σ is the vector of sliding variables and $\tilde{f}(x)$ represents the inherent non-linearities of the system, while satisfying the matching condition.

As discussed in (8) the proposed control law in this case is

$$u = (SB)^{-1}(\Phi S)x - \rho(SB)^{-1}\frac{P\sigma}{\|P\sigma\|} \tag{17}$$

and to verify stability, S can be chosen as $S = diag([I_x, I_y, I_z])$ from where it follows that $SB = I_{3\times3}$.

By making a choice of $\Phi = -\frac{1}{2}I_{3\times3}$ the solution of the Lyapunov equation (11) yields $P = I_{3\times3}$ as well. Using the same Lyapunov candidate function as stated before, $V = \sigma^T P\sigma$, it follows that

$$\dot{V} \leq \|\sigma\|^2 - 2\gamma\|P\sigma\| < 2\gamma\|\sigma\| = 2\gamma\sqrt{V} < 0 \tag{18}$$

where $\gamma = \rho - c > 0$. Therefore the control law proposed here guarantess that the sliding surface will be reached in finite time, which guarantees that the x-dynamics reach zero in finite time.

The sign function $sgn(x) = \frac{x}{\|x\|}$ which is used throughout the non-linear part of the control law is discontinuous and thus makes the whole control law discontinuous. This effect can be mitigated by switching to a different function that serves an equivalent purpose such as $tanh(x)$, or by approximating the sign function as

$$sign(x) = \frac{x}{\|x\| + \epsilon} \tag{19}$$

where $\epsilon > 0$ and $\epsilon << 1$

4 Control allocation

Control allocation refers to the problem of dividing the control input demanded by a controller to the available actuators in the system, and appears when simulating a controlled, overactuated system. However, given that the control law discussed in the previous section is designed to produce torques as outputs, there is a need to translate these torque demands to spacecraft systems actuation. In this work it is presumed that gas thrusters are available, which are able to provide fixed amounts of thrust in all three primary axes directions in the spacecraft's body frame, as well as the negative directions of these axes, for a total of 6 thrusters.

In order to solve the thruster allocation problem, first a representation of the thrust capabilities of the spacecraft is crafted as follows: a $3 \times N$ matrix is constructed, where N is the total number of available thrusters, and whose i-th column represents the torque vector that the i-th thruster would exert to the spacecraft body, if fired. Supposing available thrusters in both positive and negative directions of the primary axes, of the same thrust magnitude, A can be defined as follows:

$$A = \begin{bmatrix} 1 & 0 & 0 & -1 & 0 & 0 \\ 0 & 1 & 0 & 0 & -1 & 0 \\ 0 & 0 & 1 & 0 & 0 & -1 \end{bmatrix} \tag{20}$$

The first step in the proposed solution is to check that the dimensions of the span of its columns, i.e. the rank of the matrix. If it holds that $rank(A) = 3$, then there exists a linear combination of the vectors represented as matrix columns that will generate any possible vector in $\mathbb{R}^3$. Further checks should be performed to verify that there exists a solution for every $b \in \mathbb{R}^3$ of the problem $A\bar{x} = \bar{b}$ where $0 \leq \bar{x}$, i.e. if positive combinations of the vectors represented as columns of A still span the $\mathbb{R}^3$ vector space [12]. In any case, in the definition given in (20) this is trivial to prove. After defining the A matrix, then the iterative approach of linear least squares is used to solve the system of equations via following optimisation problem:

$$\begin{aligned} &min\|A\bar{x} - \bar{b}\| \\ &s.t. \qquad 0 \leq \bar{x} \end{aligned} \tag{21}$$

This optimisation, given that $\|A\tilde{x} - \bar{b}\| \to 0$, produces a vector $\bar{x}$ which represents the (nonnegative) percentage of torque required by each of the available thrusters, so that when all the individual torques are combined they will generate the total torque $\bar{b}$. However, since an upper bound for $\bar{x}$ is not defined, there is a possibility for some $\bar{x}_i > 1$. To mitigate this problem this vector is scaled by a factor of $max(x_i)$ in such a case, thus producing a vector $\tilde{x}$ such that:

$$\tilde{x} = \begin{cases} \frac{\bar{x}}{max(x_i)} & max(x_i) > 1 \\ \bar{x} & otherwise \end{cases} \quad (22)$$

By the definition of $\tilde{x}$, it follows that

$$A\tilde{x} = \lambda\bar{b}, \lambda \in (0, 1] \quad (23)$$

The procedure outlined above produces a vector $\tilde{x}$ of feasible torque percentages ($0 \leq x_i \leq 1$) to be commanded to each thruster, given the spacecraft's particular thruster configuration. Nevertheless, as is easily deductible from (23), in cases where the feasible output is scaled, it remains parallel to the initial target vector $\bar{b}$. Given the on-off nature of gas thrusters, in order to accommodate cases where $x_i \notin \{0, 1\}$ a pulse-width modulation (PWM) technique is used. Given the spacecraft's nonzero moments of inertia around its principal axes, its body will act as a low-pass filter to thruster pulses given a high enough pulse frequency. To generate the PWM signals for each thruster, we define a function $f_{PWM}(x, t)$ as follows:

$$f_{PWM}(x, t) = \begin{cases} 1, & \frac{1}{T}mod(t, T) < x \\ 0, & otherwise \end{cases} \quad (24)$$

where $\frac{1}{T}$ is the frequency of the PWM carrier. Then, a function $\tilde{f}_{PWM}(\tilde{x}, t)$ can be defined as follows:

$$\tilde{f}_{PWM} = \begin{bmatrix} f_{PWM}(x_1, t) & f_{PWM}(x_2, t) ... f_{PWM}(x_N, t) \end{bmatrix}^T \quad (25)$$

And thus, the technique outlined in this subsection allows one to use the expression $A\tilde{f}_{PWM} = \bar{M}$ in the dynamics equation (4).

5 Simulation results

5.1 Preliminaries

For simulation purposes of the above, a spacecraft with $I = diag([100, 55, 60])$ is used along with a constant ρ parameter appropriately selected. Furthermore, to enhance the realism of the simulation, the state vector of the spacecraft dynamics is sampled at a constant rate of 10Hz and is then fed back to the controller in order to mimic intermittent readings from onboard sensors.

Given that the thrusters are mechanical systems with a finite response time, one extra step towards a realistic simulation is to imitate this inertia in their actuation. To this end, all PWM inputs to the thrusters are being passed to a simple low-pass filter block before being handed over to the dynamics block. The transfer function used for this is as follows:

$$G(s) = \frac{\omega_0}{s + \omega_0} \quad (26)$$

where the value of ω_0 can be chosen so the filter corresponds better to response rates of a particular thruster model.

The effect that this filter has on thruster actuation is twofold; it limits the actuation speed so it is not instantaneous, and it hinders the ability of the thrusters to respond to pulses with either too low or too high of a duty cycle percentage.

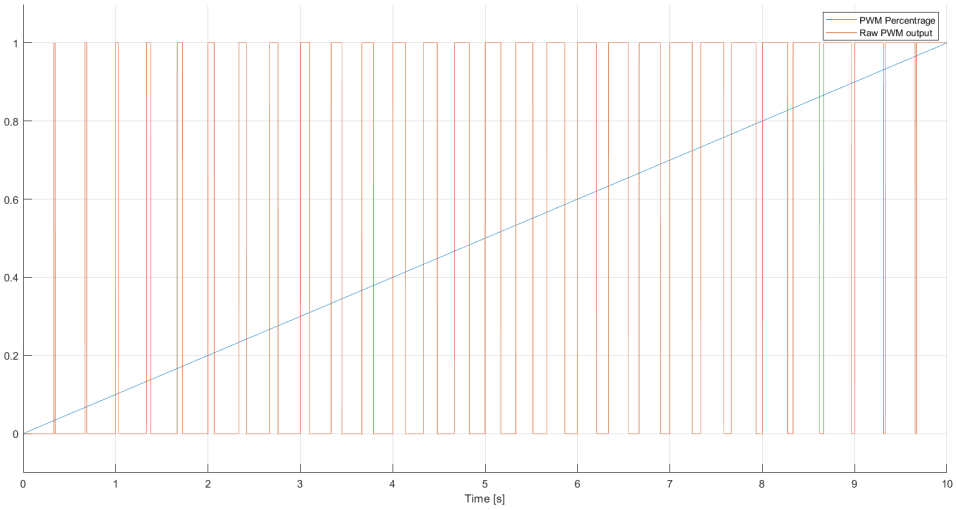

Fig. 1 PWM signal generation

In Figure 1 the PWM generating function is verified with a simple duty cycle ramp as input, and a selected PWM frequency of 3Hz. The reader can notice that the output of this function is discontinuous and if used as is would presume immediate response from the thrusters.

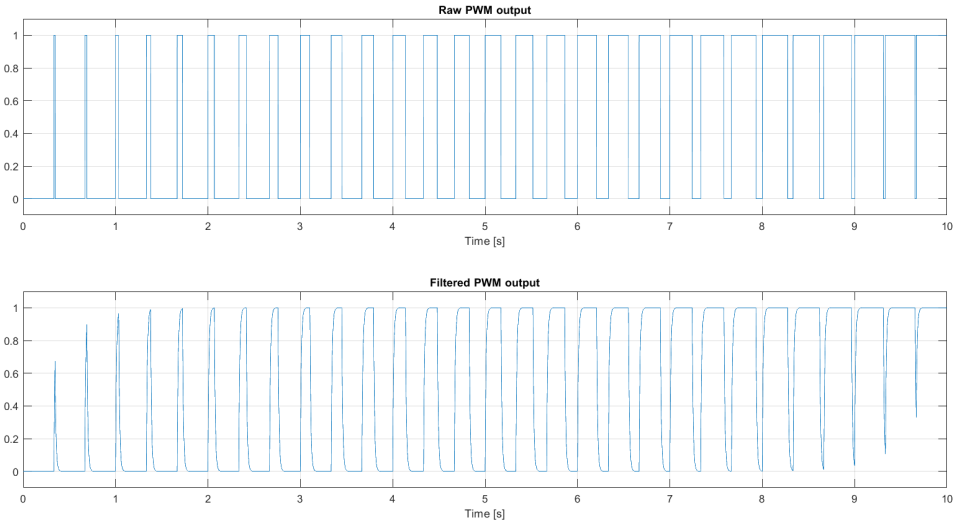

Fig. 2 Raw PWM vs Filtered thruster actuation

In Figure 2 the smoothing effect of the low-pass filter can be seen. For small duty cycle values (ie. around t = 0-1s) the response of the attenuated actuators prevents them from achieving a fully on state, whereas on high duty cycle values (ie. around t = 9-10s) the opposite is true and the actuators are prevented from completely turning off.

5.2 Stability of dynamics

To verify the stability of the dynamics under the proposed control law, the simulated spacecraft is set to have an initial arbitrary set of angular rates and the controller is driving the dynamics to zero in finite time. Sampling frequency for state variables is set to $10Hz$, and the PWM frequency is defined at $5Hz$, and $\rho = 2$

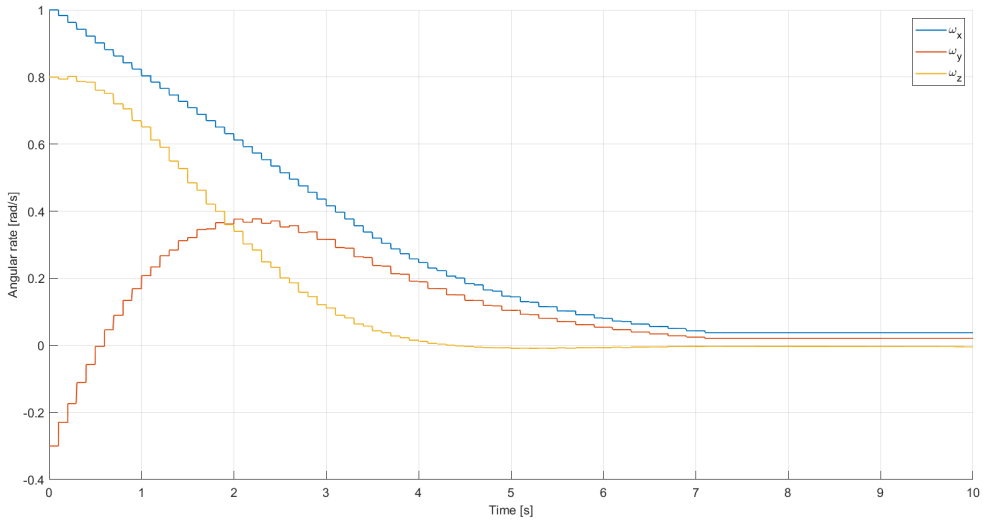

Fig. 3 Dynamics stability

In Figure 3 we can see that despite the intermittent state updates and the PWM affecting the angular rates in discrete steps, the proposed control law manages to stabilise the dynamics in finite time. The control effort, translated to actuator inputs, can be seen in Figure 4. The steady-state error which is present after the stabilisation ($t > 7s$) is due to the filtering action of the low-pass stage that prevents small duty cycles from being translated to actual pulses. The discontinuity in the slope of the thruster curves can be attributed to the sampling rate that is being used to feed the controller with state information.

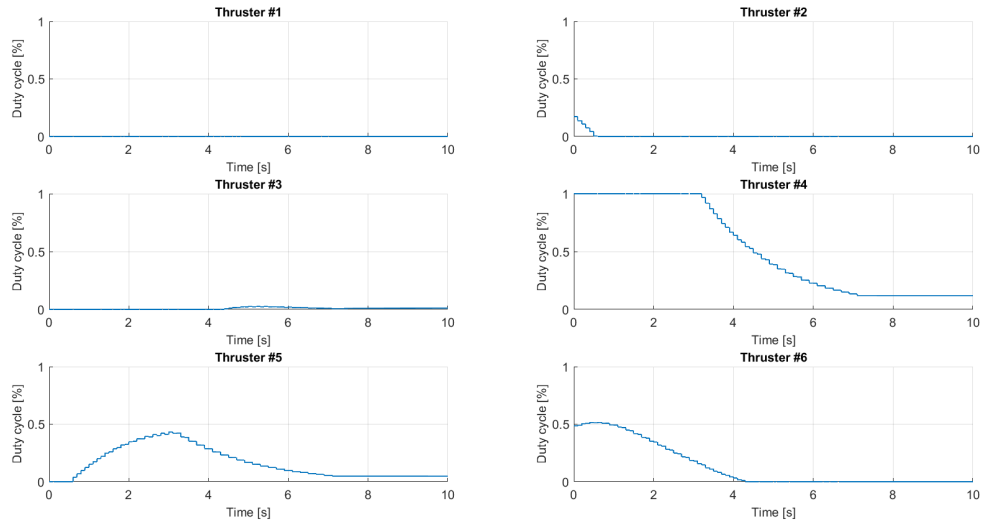

Fig. 4 Thruster duty cycles

Leaving the simulation as defined previously, control performance under different values of ρ are shown in Figure 5, Figure 6. As was expected by Equation 10 and shown by simulation results in Figure 7, different values of ρ affect the performance of the control law by means of affecting the demanded torques the control law outputs. While this approach may be used to alleviate the steady-state error, in the zoomed part of Figure 6 it is evident that this induces chattering when combined with the "dead-band" that is produced by the low-pass filtering of the PWM signals. The chattering is evident in Figure 8, in which it it shown that opposing thrusters being fired sequentially while the spacecraft is near stabilisation and the demanded torques fall within the actuation dead-band.

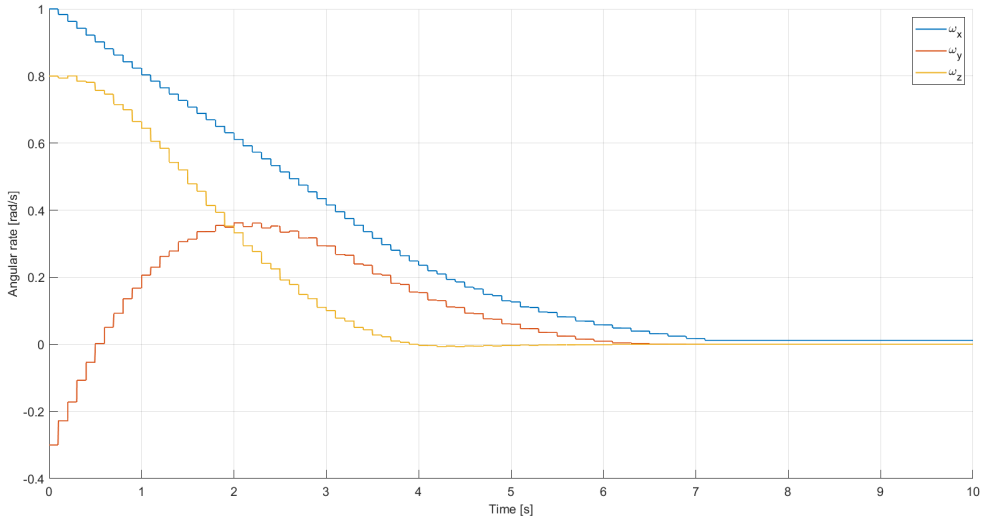

Fig. 5 Dynamics stability at $\rho = 0.5$

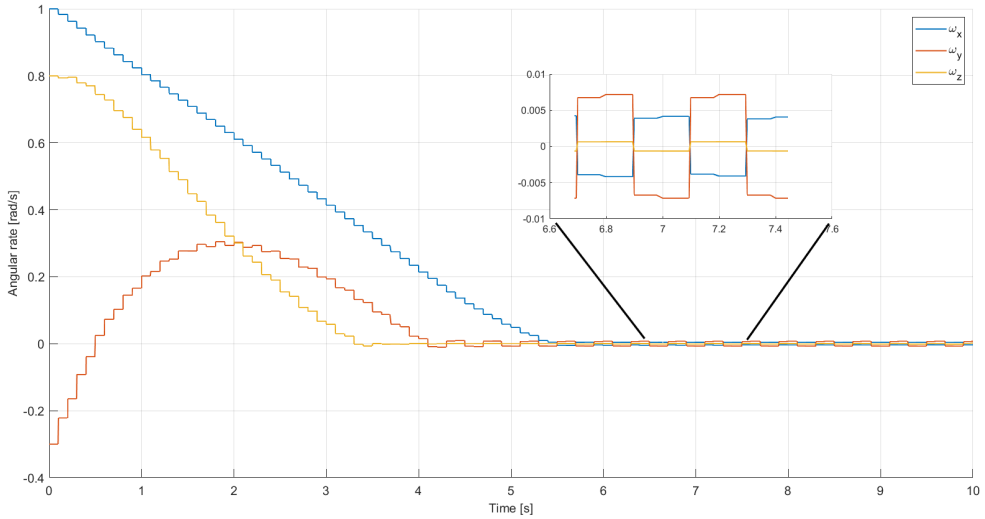

Fig. 6 Dynamics stability at $\rho = 0.1$

Thus, an optimal value of ρ may be chosen so as to minimise the steady-state error while avoiding the introduction of control chattering for a given system.

5.3 Performance under disturbance

Continuing with the performance trials, leaving the simulation parameters unchanged and with an optimal value of ρ selected through trial and error for the particular system, a disturbance torque is

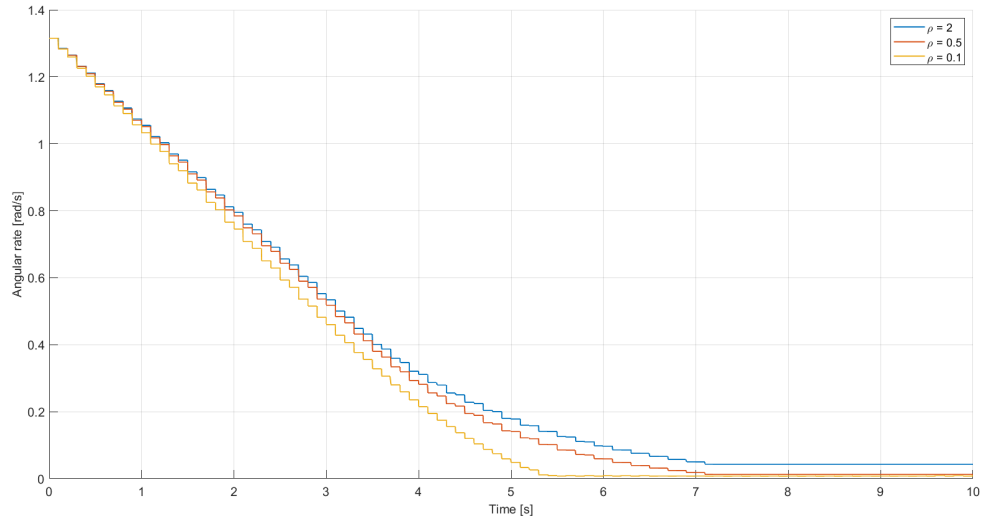

Fig. 7 Performance under different ρ values

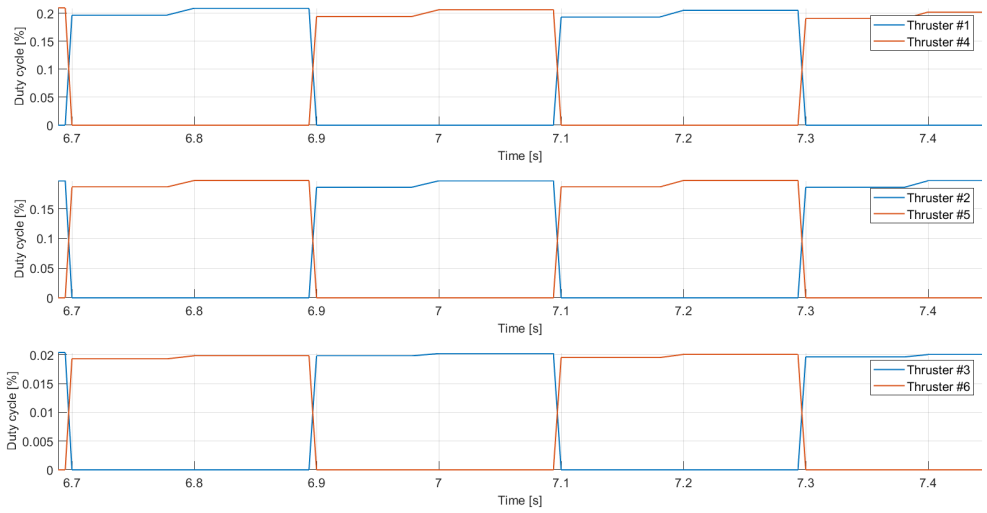

Fig. 8 Chattering effect / competing thrusters at $\rho = 0.1$

introduced in the spacecraft's dynamics. In the payload deployment case, this disturbance would occur when the spring-release mechanisms are actuated and the payload is pushed away from the carrier spacecraft. To simulate this effect, a randomised disturbance torque is injected that is $10x$ the magnitude of the total thrust available by the actuators. The disturbance is enveloped by a gaussian function with minimal spread ($\sigma = 0.1$) to mimic the almost instantly rising and subsequently rapidly declining torque impacted on the spacecraft. After the disturbance injection, the inertia tensor is changed to $0.9I_0$ to reflect the result of mass being ejected, while the control law remains unchanged. The pertinent results are shown Figure 9 and Figure 10, in which the control law shows the capability of handling the disturbance and stabilising the spacecraft.

5.4 Attitude tracking

Given the robust performance of the controller for tracking the nonlinear dynamics of attitude, such a control law might be used in a two-stage overall control architecture for attitude tracking. To this end,

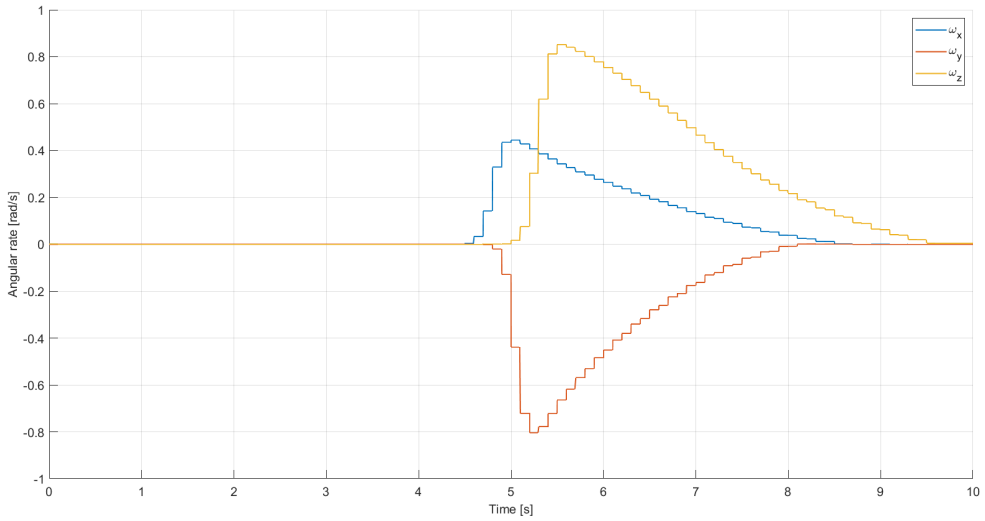

Fig. 9 Angular rates under disturbance

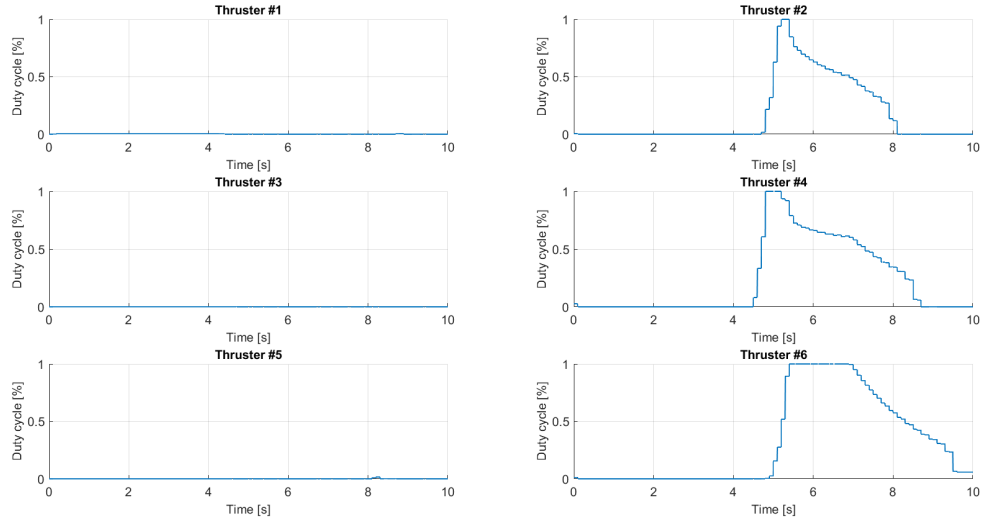

Fig. 10 Thruster duty cycles under disturbance

an attitude reference of Euler angles is created emulating a spacecraft in a low eccentricity orbit, which would imply tracking a sinusoidal reference for attitude.

For a proof of concept, a simple PID controller was used to determine the attitude error and generate angular rates which are in turn fed to the sliding mode controller for tracking. An arbitrary initial attitude error is selected, and the disturbance is injected at an appropriate time after the initial error dynamics stabilisation. The tracking performance of the compound controller is presented in Figure 11 and Figure 12.

As can be seen in Figure 11, a compound-control approach can handle the tracking of attitude angles given a reference and still show enough robustness against sudden external disturbances. However, by taking a look at Figure 12, the reader can identify a potential problem in the continuous usage of thrusters. Given the premise of this simulation this isn't required, since the requirement is for tracking of relatively constant angular rates.

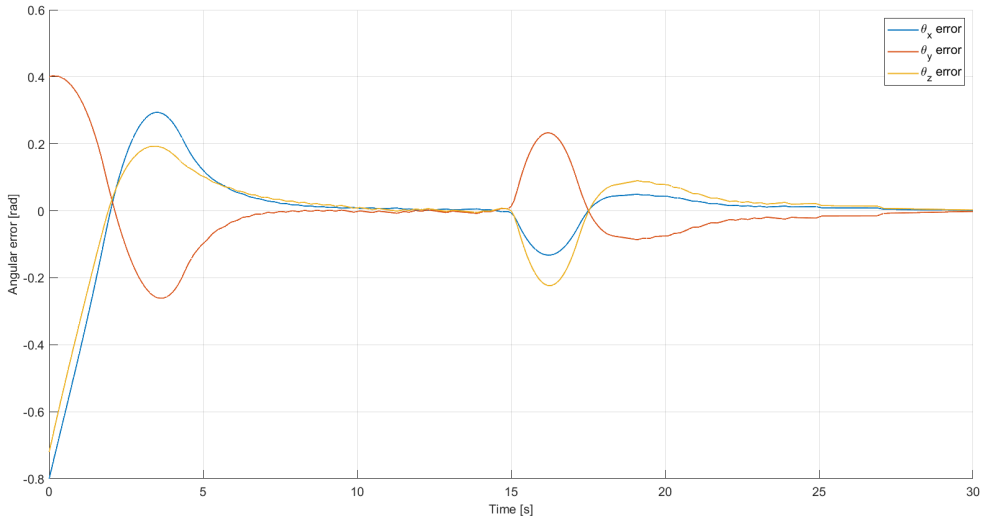

Fig. 11 Compound tracking controller - Error dynamics

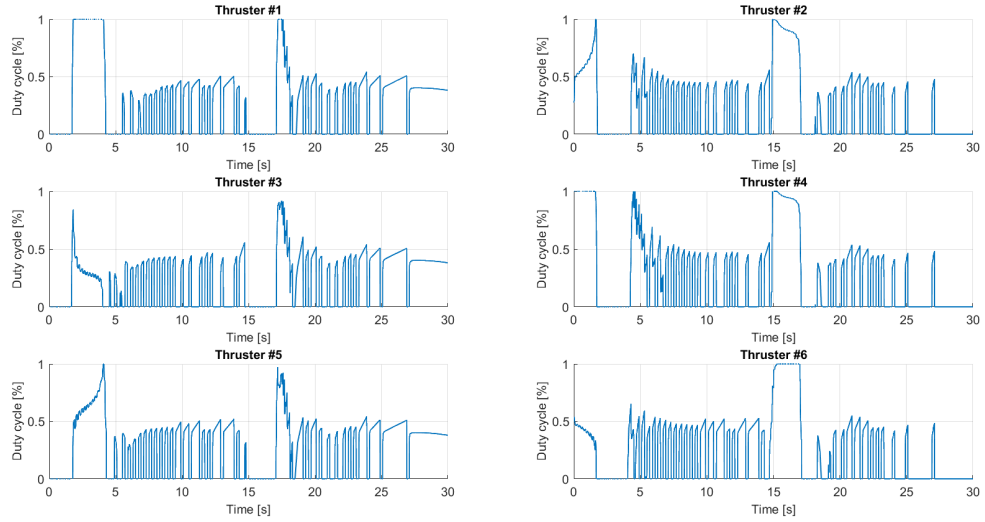

Fig. 12 Compound tracking controller - Thruster actuation

6 Conclusions

In this work, the feasibility of using a first order sliding mode control law, designed under the matched uncertainty principle, for stabilising the dynamics of a spacecraft has been proven theoretically by means of Lyapunov theory, and demonstrated with a realistic model of spacecraft dynamics, actuation and control. The control law used herein is not constrained by linearisations about operating points, and the stability of the controller has been verified in the presence of external disturbances, which would manifest in the case of orbital payload deployment by means of reaction torques on the carrier spacecraft. The tune-ability of such a controller's response and the change in the performance characteristics has been shown with varying selection of design-time parameters.

Moreover, given the good performance of angular rate tracking by the sliding mode controller, a proof-of-concept second simulation with a compound controller has been set up to demonstrate the possibilities of attitude tracking. This approach would require further investigation, in particular crafting a control law that takes into consideration both attitude angles and rates as a reference, in order to minimise chattering of the system actuators when target attitude has been reached given requirements

of tracking low frequency rates. Additionally, inclusion of other types of actuators in the model (e.g., reaction wheels) and implementation of an appropriate control allocation strategy depending on error magnitude would be highly beneficial in this case.

Apart from the already mentioned points, future work on this subject would include incorporating control elements regarding orbital dynamics and station keeping, or general orbital maneuvering situations. The extendability of the proposed SMC law might prove to be difficult without resorting to higher order controllers, but this will be determined on a case-by-case basis depending upon new results.

Acknowledgments

This work was supported by Coactum SA, through the Cranfield University Industrial Partnership Framework. Apart from the financial support, the authors would like to also acknowledge the helpful insights and advice from the AOCS team of Coactum SA.

References

[1] Alexander S. Poznyak and Yury V. Orlov. Vadim i. utkin and sliding mode control. *Journal of the Franklin Institute*, 360(17):12892–12921, 2023. ISSN: 0016-0032. DOI: 10.1016/j.jfranklin.2023.09.028.

[2] Dongjun Shin and Jinho Kim. Robust spacecraft attitude control using sliding mode control. In *Guidance, Navigation, and Control Conference and Exhibit*, page 4432, 1998. DOI: 10.2514/6.1998-4432.

[3] Kunfeng Lu, Yuanqing Xia, Zheng Zhu, and Michael V Basin. Sliding mode attitude tracking of rigid spacecraft with disturbances. *Journal of the Franklin Institute*, 349(2):413–440, 2012. DOI: 10.1016/j.jfranklin.2011.07.019.

[4] Fuyuto Terui. Position and attitude control of a spacecraft by sliding mode control. In *Proceedings of the 1998 American Control Conference. ACC (IEEE Cat. No. 98CH36207)*, volume 1, pages 217–221. IEEE, 1998. DOI: 10.1109/ACC.1998.694662.

[5] Chutiphon Pukdeboon and Poom Kumam. Robust optimal sliding mode control for spacecraft position and attitude maneuvers. *Aerospace Science and Technology*, 43:329–342, 2015. DOI: 10.1016/j.ast.2015.03.012.

[6] Haichao Gui and George Vukovich. Adaptive integral sliding mode control for spacecraft attitude tracking with actuator uncertainty. *Journal of the Franklin Institute*, 352(12):5832–5852, 2015. DOI: 10.1016/j.jfranklin.2015.10.001.

[7] Hyochoong Bang, Cheol-Keun Ha, and Jin Hyoung Kim. Flexible spacecraft attitude maneuver by application of sliding mode control. *Acta Astronautica*, 57(11):841–850, 2005. DOI: 10.1016/j.actaastro.2005.04.009.

[8] Shijie Xu, Naigang Cui, Youhua Fan, and Yingzi Guan. Flexible satellite attitude maneuver via adaptive sliding mode control and active vibration suppression. *AIAA Journal*, 56(10):4205–4212, 2018. DOI: 10.2514/1.J057287.

[9] Ang Li, Ming Liu, and Yan Shi. Adaptive sliding mode attitude tracking control for flexible spacecraft systems based on the takagi-sugeno fuzzy modelling method. *Acta Astronautica*, 175:570–581, 2020. ISSN: 0094-5765. DOI: 10.1016/j.actaastro.2020.05.041.

[10] David B. Guttler. *Satellite Attitude Control Using Atmospheric Drag*. PhD thesis, US Air Force Institute of Technology, Wright-Patterson AFB, OH, USA, Mar. 2007.

[11] Kiyona Miyamoto, Toshihiro Chujo, Kei Watanabe, and Saburo Matunaga. Attitude dynamics of satellites with variable shape mechanisms using atmospheric drag torque and gravity gradient torque. *Acta Astronautica*, 202:625–636, 2023. ISSN: 0094-5765. DOI: 10.1016/j.actaastro.2022.11.014.

[12] Chandler Davis. Theory of positive linear dependence. *American Journal of Mathematics*, 76(4), October 1954. DOI: 10.2307/2372648.